Effects of Operating Conditions on Longitudinal Solids Mixing in a Circulating Fluidized Bed Riser

M. J. Rhodes, S. Zhou, T. Hirama, and H. Cheng
Dept. of Chemical Engineering, University of Bradford, Bradford, England

Longitudinal solids mixing was studied experimentally in circulating fluidized bed risers of internal diameter 0.152 m and 0.305 m. Superficial gas velocity and mean solids flux used were 2.8–5.0 m/s and 5.0–80 kg/m^2·s, respectively, and the bed solids had a surface volume mean diameter of 71 μm and a particle density of 2,456 kg/m^3. A sodium chloride tracer was used in impulse injection experiments. A simple, one-dimensional dispersion model describes measured solids mixing satisfactorily. Peclet numbers (U_oL/D_z) found, in the range 1.0–9.0, were correlated with the riser diameter and mean solids flux. The modeling approach described here permits residence time distribution curves to be calculated directly from the knowledge of superficial gas velocity, mean solids flux, and riser diameter. Longitudinal solids mixing in the riser decreased with increasing riser diameter. The results are consistent with recent hydrodynamic studies.

Introduction

In recent years, much attention has been focused on the circulating fluidized bed (CFB). The main application of this technology is at present in the combustion of low-grade fuels to strict environmental standards. However, the strong similarity between fluid dynamic conditions in the riser of a circulating fluidized bed and those in the riser transport reactor has attracted the attention of the oil industry to the recent studies of CFB fluid dynamics. The common flow pattern is characterized by a rapidly-rising, dilute gas-particle suspension in the core of the riser surrounded by a slowly-falling, denser suspension in the region adjacent to the riser walls. This flow regime has been described as refluxing dilute-phase transport (Rhodes, 1989) and in circular risers has become known as the core-annulus flow. Information on the solids motion and residence time distribution in this flow regime is of vital importance to the reactor design and the fluid dynamics.

Several previous studies of solids mixing are relevant. Avidan (1980) and Yerushalmi and Avidan (1985) made residence time distribution (RTD) measurements using a ferromagnetic tracer and an inductance bridge detector. These authors applied the one-dimensional dispersion model of Levenspiel and Smith (1957) to obtain measures of solids diffusivity. Helmrich et al. (1986) reported a double-peak RTD in their experiments using a radioactive solids tracer. Bader et al. (1988) used sodium chloride as the tracer that was detected by dissolving in water and by measuring electrical conductivity. Their single-peak residence time distributions indicated a high degree of solids backmixing in the wall region and a substantial transfer of solids between riser core and wall regions. In this work, we used an experimental technique based on that of Bader and coworkers (1988) and studied the effect of superficial gas velocity, mean solids flux, and riser diameter on the longitudinal solids mixing in the CFB riser.

Experimental Studies

CFB apparatus

The form of circulating fluidized bed apparatus used in these experiments is shown in Figure 1. The apparatus shown in the figure is the smaller of two used in experiments and has a riser with an internal diameter of 152 mm and 6.2 m high. Air from a Rootes-type blower is fed to the riser through a distributor consisting of a packed bed of glass balls. The flow of particulate solids from the solids reservoir to the base of the riser is controlled by a 100-mm-diameter *L*-valve. At the exit of the riser, solids are separated from air by two stages of cyclone separation and returned to the solids reservoir. Solids circulation rate is determined by diversion of the solids leaving the primary cyclone (>99% efficient) into another vessel known as the

T. Hirama is presently with Government Industrial Development Laboratory, Sapporo, Hokkaido, Japan.

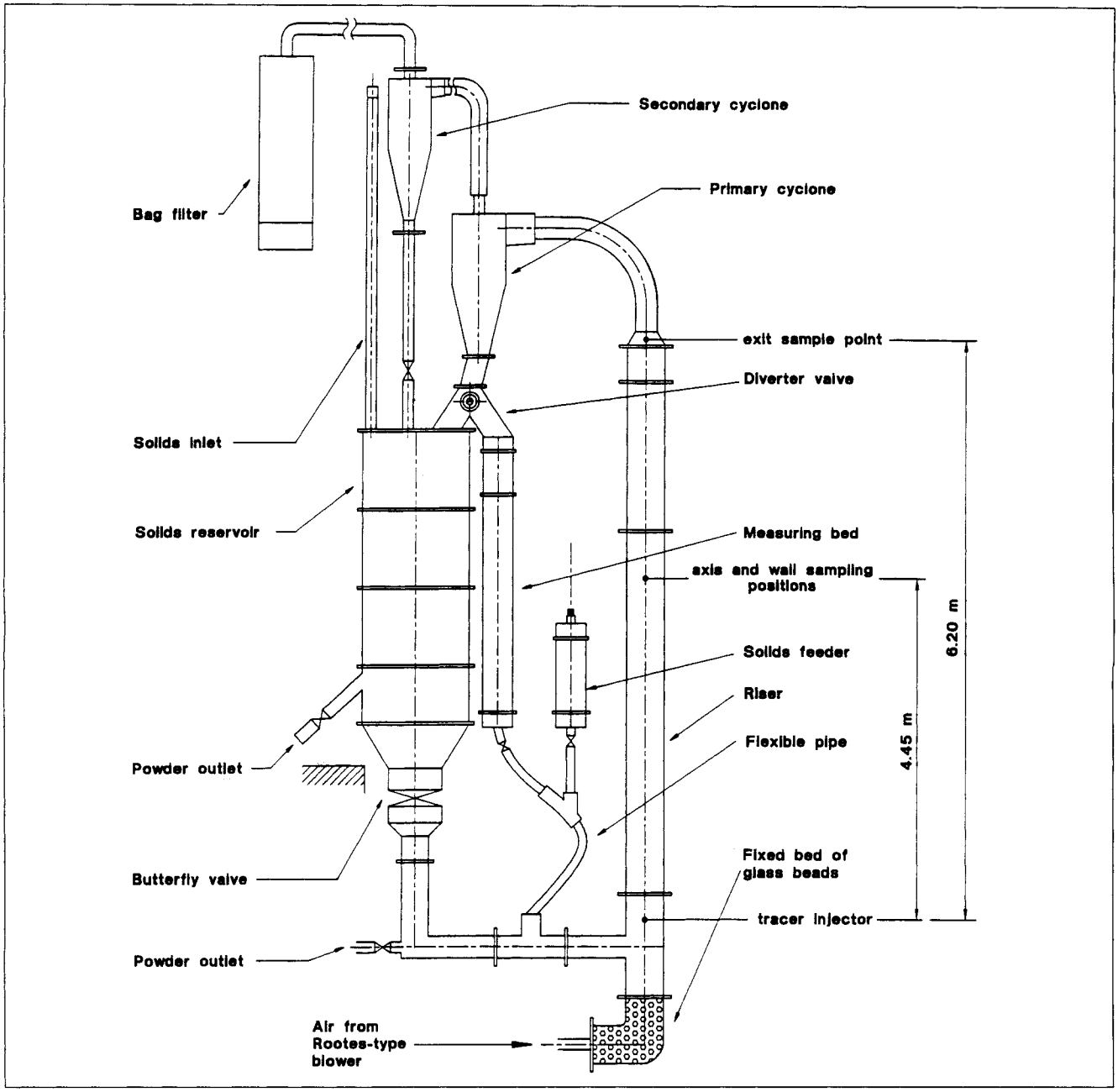

Figure 1. Smaller circulating fluidized bed cold model.

measuring bed for a measured time. By fluidizing the solids in this measuring bed it is possible to determine the weight of the diverted solids. Diverted solids can be returned to the main system while the apparatus is in operation. The positions of the tracer injector and the sampling points are shown in Figure 1. The larger CFB apparatus used in these experiments was similar in form to that shown in Figure 1 but had a riser internal diameter of 305 mm, a riser height of 6.60 m, L-valve diameter of 152 mm, and a reservoir diameter of 900 mm. The axis and wall sampling points were 4.2 m above the injector, and the exit sampling point was 6.6 m above the injector. The powder circulated in both CFB rigs was FRF5, a nonporous alumina with a particle density of 2,456 $kg \cdot m^{-3}$, and a size distribution shown in Table 1.

Table 1. Size Distribution of FRF5 Powder and Salt Tracer*

FRF5 Powder		NaCl Tracer	
Size Range (μm)	Undersize Range (%)	Size Range (μm)	Undersize Range (%)
125–150	100	125–150	100
90–125	99.2	90–125	99.5
63–90	78.8	63–90	86.9
38–63	28.7	38–63	49.3
0–38	4.8	0–38	25.0

*Surface-volume mean sizes FRF5: 71 μm.

Solids mixing measurements

The method described below is based on that described by

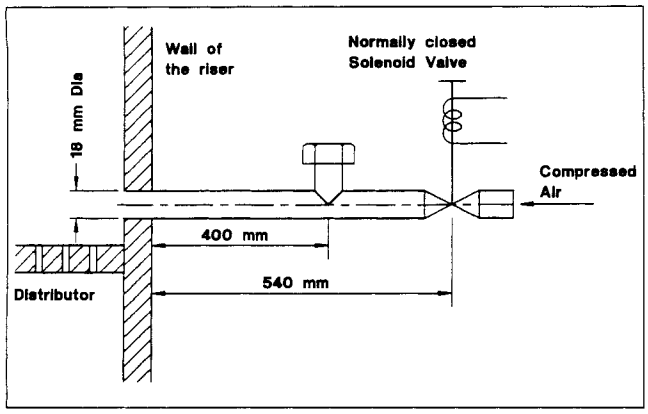

Figure 2. Tracer injection arrangement

Bader et al. (1988). The solids tracer used in the mixing experiments was sodium chloride ground to give a size distribution similar to that of the FRF5 powder used as bed solids (see Table 1). The particle density of the sodium chloride (2,160 $kg \cdot m^{-3}$) was acceptably close to that of the FRF5 powder. The tracer injection system is shown in Figure 2. Preliminary tests using a high-speed video recording system demonstrated that using this system, the required quantity of tracer could be injected in less than one second. The compressed air used to inject the tracer was found to increase air flow in the riser by only 3–8%.

Tracer sampling was performed simultaneously at three locations in the riser, shown in Figure 1. Each location was equipped with the sampling system shown in Figure 3. The sampling tubes used at the riser center and exit locations were 7.5-mm-ID tubes bent at 90° and pointing upstream. Sampling at the riser wall location was done by positioning a 7.5-mm sampling tube with its tip flush with the inside surface of the riser wall. Immediately before sampling, all sampling lines were purged with barely sufficient air to prevent ingress of bed solids. The solenoid valves indicated in Figures 2 and 3 permitted sampling to start at all three riser locations simultaneously with injection of the sodium chloride tracer.

Sampled solids were discharged from the cyclone dipleg into a series of containers with the aid of slight pressure applied to the gas exit of the cyclone. This permitted solids to be recovered from the dipleg with minimum axial mixing. The samples collected in the containers were each weighed and then washed with 100 mL of deionized water. After ensuring that all the tracer in the sample was dissolved, the conductivity of the resulting solutions was measured. The concentration of each solution and, hence, mass of tracer in each sample was then found from a prior calibration of conductivity vs. concentration of a tracer solution. Thus, records of the variation in mass of tracer collected with time at each riser location were

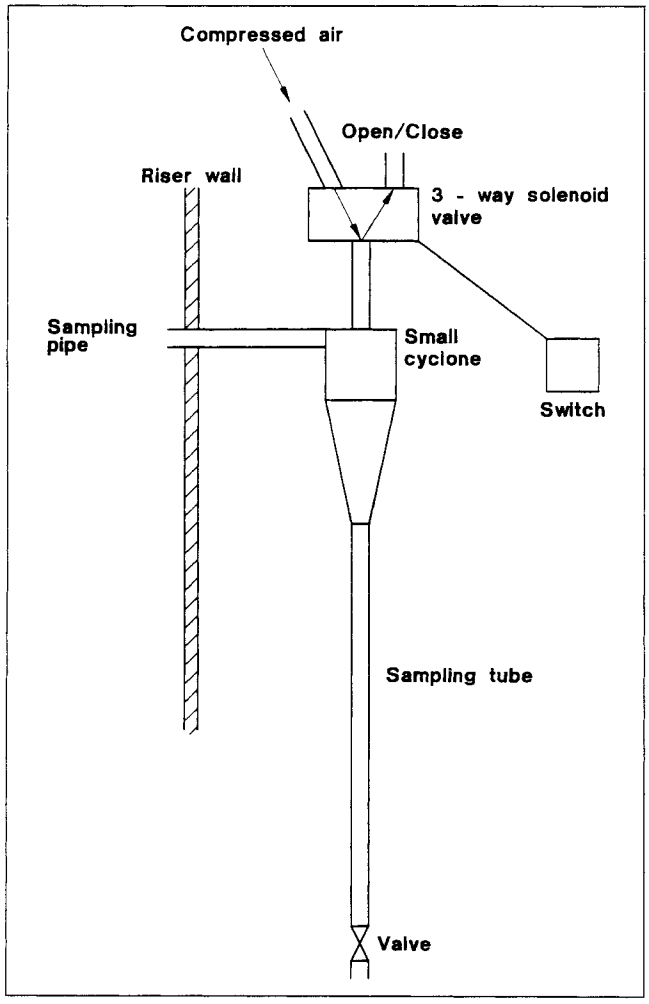

Figure 3. Sampling system.

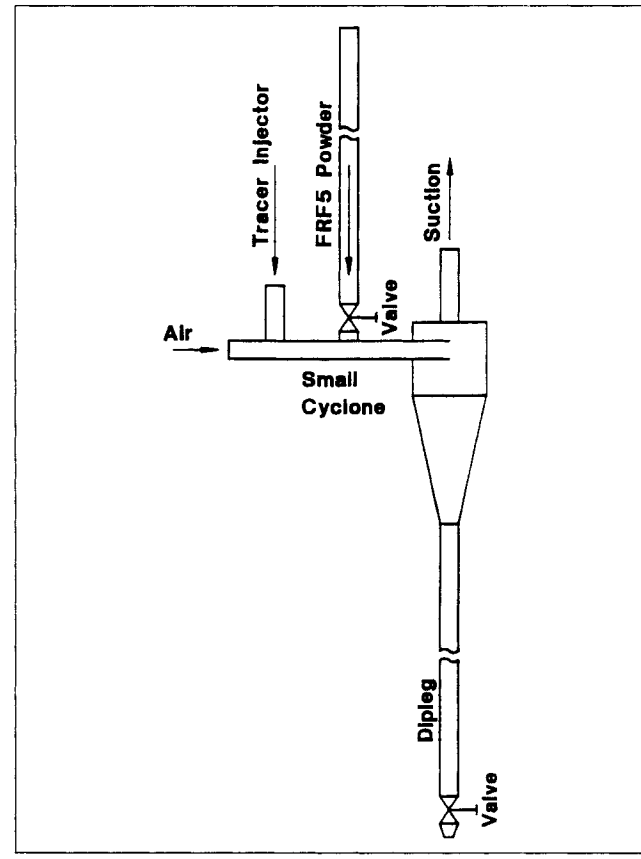

Figure 4. Apparatus for determination of experimental error in sampling method.

Table 2. Solids Mixing Data: Experimental Conditions and Results on 0.152-m Rig*

Conditions of Experiment		$U_o = 2.81$ m/s $G_s = 29.4$ kg/m^2·s $D = 0.152$ m				Conditions of Experiment		$U_o = 4.02$ m/s $G_s = 29.6$ kg/m^2·s $D = 0.152$ m				Conditions of Experiment		$U_o = 5.00$ m/s $G_s = 29.6$ kg/m^2·s $D = 0.152$ m			
Positions of the Probes						Positions of the Probes						Positions of the Probes					
$r = 0$ m $L = 6.20$ m		$r = 0$ m $L = 4.45$ m		$r = 0.073$ m $L = 4.45$ m		$r = 0$ m $L = 6.20$ m		$r = 0$ m $L = 4.45$ m		$r = 0.073$ m $L = 4.45$ m		$r = 0$ m $L = 6.20$ m		$r = 0$ m $L = 4.45$ m		$r = 0.073$ m $L = 4.45$ m	
t	C	t	C	t	C	t	C	t	C	t	C	t	C	t	C	t	C
0.4	0.3	0.2	0	0.2	0	0.3	0	0.3	2.9	0.3	0.5	0.3	0	0.3	5.1	0.4	2.4
1.0	0.9	0.5	1.0	0.6	0	0.9	0.8	0.8	7.2	0.8	1.3	0.9	2.7	0.8	8.0	1.2	5.3
1.5	3.1	0.8	3.2	1.1	0.9	1.4	3.2	1.3	6.8	1.3	1.6	1.4	4.6	1.3	7.1	1.9	6.9
2.0	5.1	1.2	4.7	1.6	2.9	2.1	4.2	1.9	6.7	1.9	3.9	1.9	5.6	1.7	6.6	2.5	7.1
2.8	5.3	1.7	5.1	2.1	4.5	2.8	4.5	2.5	5.8	2.6	5.2	2.5	5.2	2.3	6.3	3.4	7.2
3.9	5.4	2.4	5.8	2.8	5.1	3.5	4.1	3.3	5.5	3.6	6.1	3.1	4.3	2.9	5.1	4.5	6.4
4.9	4.6	3.1	5.7	3.6	5.9	4.3	3.5	4.1	5.3	4.8	6.7	3.9	3.6	3.6	4.6	5.9	5.9
5.9	4.2	4.0	5.1	4.2	5.7	5.4	2.9	5.2	4.7	6.0	6.1	4.9	2.6	4.5	3.8	7.2	5.0
7.0	3.7	5.0	4.7	5.0	5.3	6.6	2.3	6.7	2.9	7.6	5.2	5.9	2.4	5.4	3.2	8.4	4.8
8.0	2.8	6.0	4.1	6.1	4.7	7.7	1.7	8.3	2.6	9.3	3.5	7.0	1.6	6.6	3.0	9.6	4.1
9.2	2.7	7.0	3.1	7.2	4.6	9.0	1.3	9.8	1.9	11.0	3.5	8.1	1.1	8.0	2.5	10.8	4.0
10.4	2.7	8.1	2.9	8.3	3.8	10.4	1.2	11.1	1.4	12.6	3.0	9.1	1.0	9.2	2.0	12.1	3.1
11.6	1.5	9.3	2.3	9.5	3.5	11.7	0.9	12.5	1.4	14.0	2.5	10.2	0.9	10.3	1.7	13.4	2.6
12.8	1.3	10.7	2.0	10.7	2.8	13.1	0.8	13.9	1.2	15.5	2.1	11.4	0.7	11.5	1.3	14.8	1.9
14.0	0.8	12.1	1.7	11.9	2.3	14.5	0.8	15.3	1.1	17.0	1.9	12.6	0.5	12.7	1.1	16.1	2.0
15.3	0.8	13.4	1.5	13.3	2.2	16.0	0.4	16.6	0.5	18.4	1.6	13.6	0.4	14.0	0.9	17.3	1.8
16.5	0.5	14.6	1.4	14.7	1.7	17.3	0.3	18.0	0.5	19.9	1.4	14.6	0.5	15.3	0.8	18.6	1.8
17.6	0.5	16.0	0.9	16.2	1.5	18.6	0.3	19.5	0.5	21.3	1.2	15.7	0.5	16.6	0.8	19.8	1.8
18.8	0.4	17.2	0.7	17.5	1.3	19.9	0.3	20.9	0.6	22.8	1.0	16.6	0.5	17.7	0.8	21.2	1.0
20.0	0.4	18.5	0.6	19.0	1.0	21.3	0.3	22.3	0.5	24.3	1.0	17.7	0.4	18.8	0.7	22.6	1.0
21.1	0.1	20.1	0.6	20.5	0.9	22.5	0.2	23.9	0.5	25.9	1.1	18.8	0.4	20.1	0.7	24.2	0.9
22.4	0.2	21.9	0.3	21.9	0.7	23.7	0.2	25.7	0.5	27.7	0.8	20.3	0.2	21.5	0.4	25.8	1.3
23.8	0.1	23.8	0.3	23.3	0.3	25.4	0.1	27.4	0.5	29.5	0.8	22.4	0.2	22.8	0.4	27.4	0.9
25.5	0.2	25.6	0.3	24.6	0.7	27.7	0.1	29.2	0.6	31.0	0.8	24.5	0.2	24.4	0.4	28.9	0.9
27.1	0	27.2	0.3	26.2	0.3	30.3	0	31.3	0.5	32.6	0.9	26.3	0.2	26.5	0.4	—	—
28.4	0	28.5	0	28.0	0.6	32.9	0	33.3	0.5	33.7	0.8	28.4	0	28.6	0.4	—	—

*C = tracer concentration in mg-NaCl/g-FRF5
t = residence time in seconds

obtained. The error introduced by mixing in the cyclone, cyclone dipleg, and sample dividing process was estimated in a separate series of tests, in which very short pulses of tracer were injected directly into the sampling systems operating under typical sampling conditions (see Figure 4). The dipleg solids were then processed by the procedure described above to determine the variation of tracer concentration with time. The variance of the resulting distribution of tracer residence times was taken to be a measure of the absolute error caused by the sampling system. This typically gave rise to a relative error of 1–7% in the mixing experiments described here.

Results

More than 30 sets of solids mixing measurements were conducted with the CFB apparatus at Bradford under various operating conditions. Some examples with 0.152-m-dia. riser are listed in Tables 2 and 3, and some with 0.305-m-dia. riser in Tables 4 and 5. Since it is difficult to assess the effect on solids mixing of riser operating conditions and scale from the raw data presented here, it is necessary to apply a suitable analysis to the data.

Treatment of Data

The motion of solids in vertical gas-particle flow under the conditions discussed here is very complex. Generally, the flow pattern consists of a dilute, rapidly-rising core surrounded by a denser, slowly-falling region near the riser walls. Although the process of axial solids mixing in such a system is quite different from molecular diffusion, in this analysis we investigate the possibility of describing the mixing phenomena using a one-dimensional dispersion model.

For unidirectional diffusion from a point source in a fluid at rest, the tracer concentration at time t and a longitudinal position z is given by:

$$C = \frac{C_o}{2\sqrt{\pi D_z t}} \exp\left[-\frac{z^2}{4D_z t}\right] \tag{1}$$

where C_o is the integration constant and D_z is the longitudinal dispersion coefficient. We may adapt this solution to the case under investigation by allowing the center point from which diffusion occurs to move at a velocity equal to the velocity of the center of gravity of the injected cloud of tracer, $V_{s,0.5}$. With this modification, Eq. 1 becomes:

$$C = \frac{C_{0.5}\sqrt{t_{0.5}}}{\sqrt{t}} \exp\left[-\frac{(L - V_{s,0.5}t)^2}{4D_z t}\right]$$

or

Table 3. Solids Mixing Data: Experimental Conditions and Results on 0.152-m Rig*

Conditions of Experiment		$U_o = 4.02$ m/s $G_s = 5.14$ kg/m^2·s $D = 0.152$ m				Conditions of Experiment		$U_o = 4.00$ m/s $G_s = 49.3$ kg/m^2·s $D = 0.152$ m				Conditions of Experiment		$U_o = 4.03$ m/s $G_s = 65.459$ kg/m^2·s $D = 0.152$ m			
Positions of the Probes						Positions of the Probes						Positions of the Probes					
$r = 0$ m $L = 6.20$ m		$r = 0$ m $L = 4.45$ m		$r = 0.073$ m $L = 4.45$ m		$r = 0$ m $L = 6.20$ m		$r = 0$ m $L = 4.45$ m		$r = 0.073$ m $L = 4.45$ m		$r = 0$ m $L = 6.20$ m		$r = 0$ m $L = 4.45$ m		$r = 0.073$ m $L = 4.45$ m	
t	C	t	C	t	C	t	C	t	C	t	C	t	C	t	C	t	C
0.7	4.7	0.7	10.7	0.8	2.1	0.3	0.1	0.2	0.8	0.2	0.5	0.2	0	0.1	0	0.2	0
1.5	7.7	2.2	9.2	2.3	13.7	0.8	2.7	0.6	4.3	0.5	0.5	0.5	0	0.4	0.3	0.7	0.5
3.4	5.7	3.9	6.6	3.8	13.2	1.3	4.7	1.1	5.7	0.9	2.2	0.8	0.1	0.8	2.6	1.2	2.3
5.2	4.8	5.6	4.8	5.2	11.7	1.8	4.9	1.6	6.1	1.4	3.0	1.3	2.8	1.1	5.4	1.9	3.6
7.1	3.3	7.2	4.1	6.8	9.0	2.4	4.9	2.1	5.7	1.8	4.1	1.9	4.0	1.6	4.7	2.5	3.8
8.7	3.0	9.0	2.7	8.4	7.7	3.1	4.3	2.5	5.3	2.3	5.1	2.7	4.1	2.3	4.6	3.1	3.9
10.3	2.2	10.9	2.6	10.1	6.1	3.9	4.2	3.3	4.7	3.0	5.3	3.7	4.2	3.0	4.2	3.9	4.5
11.9	2.0	12.2	2.4	11.5	5.9	4.9	3.4	4.4	3.2	4.0	5.5	4.9	3.7	3.8	3.2	4.7	4.0
13.8	2.0	13.5	1.8	13.0	4.7	6.0	2.4	5.3	2.4	5.4	5.1	6.2	2.7	4.8	2.6	5.6	3.4
15.8	1.3	15.3	1.4	14.7	4.3	7.1	1.9	6.2	2.3	7.2	4.0	7.7	1.6	6.0	1.4	6.8	2.1
17.6	1.1	17.1	1.0	16.5	2.7	8.5	0.9	7.2	1.8	9.0	2.9	9.5	1.3	7.2	1.0	8.1	1.8
19.5	0.8	18.8	0.9	18.3	2.1	10.0	0.7	8.4	1.4	10.5	2.2	11.2	0.7	8.4	0.8	9.5	1.1
21.3	0.7	20.8	0.6	20.0	2.0	11.4	0.4	10.0	0.8	11.9	1.5	12.9	0.5	9.6	0.5	10.8	0.9
23.2	0.5	22.9	0.6	21.5	1.7	12.9	0.4	11.6	0.6	13.4	0.9	14.5	0.4	10.8	0.5	12.3	0.7
25.2	0.3	24.8	0.3	23.4	1.6	14.3	0.2	13.2	0.6	14.9	0.9	16.2	0.4	12.0	0.1	13.7	0.5
27.0	0.2	26.6	0.3	25.4	1.3	15.8	0.1	14.7	0.3	16.3	0.8	17.9	0.3	13.2	0.1	15.1	0.1
29.0	0.3	28.2	0.1	27.1	1.1	17.3	0.1	16.2	0.3	17.8	0.6	19.7	0.1	14.4	0	16.5	0
31.3	0.1	29.8	0.1	28.6	1.1	18.7	0.1	17.9	0.4	19.4	0.6	21.5	0.1	15.6	0	17.9	0
33.4	0.1	31.6	0.1	30.1	0.8	20.1	0.1	19.6	0.3	21.0	0.6	23.3	0.1	17.0	0.2	19.4	0
35.5	0	33.6	0	31.8	0.6	22.0	0.1	21.4	0.3	22.5	0.6	25.2	0	18.3	0	21.0	0.3
—	—	35.6	0	33.6	0.5	24.1	0.2	23.5	0.3	24.0	0.6	26.9	0.2	19.7	0	22.5	0
—	—	—	—	35.6	0.4	26.1	0	25.5	0.3	25.9	0.3	28.5	0.1	21.1	0	24.1	0.1
—	—	—	—	—	—	28.0	0	27.7	0.2	27.9	0.3	29.9	0	22.6	0	25.6	0
—	—	—	—	—	—	30.1	0	29.9	0.2	30.0	0.2	—	—	24.0	0	27.1	0
—	—	—	—	—	—	31.9	0	30.1	0.2	32.5	0.2	—	—	25.5	0	28.6	0
—	—	—	—	—	—	34.2	0.1	34.4	0	34.5	0.1	—	—	27.0	0	30.0	0
—	—	—	—	—	—	—	—	—	—	—	—	—	—	28.5	0	—	—
—	—	—	—	—	—	—	—	—	—	—	—	—	—	29.9	0	—	—

*C = tracer concentration in mg-NaCl/g-FRF5
t = residence time in seconds

$$C = \frac{C_{0.5}}{\sqrt{\theta}} \exp\left[-\frac{Pe_s(1-\theta)^2}{4\theta} \right] \tag{2}$$

where $t_{0.5}$ is the travel time of the center of gravity of the tracer cloud (median resistance time):

$$\theta = \frac{t}{t_{0.5}}$$

where $C_{0.5}$ is the tracer concentration at the center of gravity of the tracer cloud, and Pe_s is the solids Peclet number ($V_{s,0.5}L/D_z$) which is related to the Peclet number based on the superficial gas velocity Pe by:

$$Pe_s = Pe \frac{V_{s,0.5}}{U_o} \tag{3}$$

The form of the RTD curve generated by Eq. 2 is shown in Figure 5, which also indicates the effect of changing the value of solids Peclet number Pe_s on the shape of RTD curves, all having a median tracer residence time, $t_{0.5} = 4$ seconds.

Results and Discussion

To investigate the suitability of this simple model it is necessary to determine values of the median tracer residence times $t_{0.5}$, the corresponding tracer concentrations $C_{0.5}$, and the median tracer velocities $V_{s,0.5}$ for each experiment. To do this, experimental data were plotted in the form of a cumulative weight distribution function defined as:

$$F(x) = \frac{\int_0^t C(t)dt}{\int_0^\infty C(t)dt} \tag{4}$$

where $C(t)$ is the residence time distribution function. Examples of the resulting curves of cumulative weight percentage undertime vs. time are shown in Figure 6, together with corresponding residence time distribution curves from which they derive.

Thus, knowing the values of $t_{0.5}$ and $C_{0.5}$ for each tracer experiment, the validity of the model could be tested and a value of Pe_s assigned to each experiment by fitting the expres-

Table 4. Solids Mixing Data: Experimental Conditions and Results on 0.305-m Rig*

Conditions of Experiment		$U_o = 40$ m/s $G_s = 20.3$ kg/m^2·s $D = 0.305$ m		Conditions of Experiment		$U_o = 4.0$ m/s $G_s = 60.3$ kg/m^2·s $D = 0.305$ m				Conditions of Experiment		$U_o = 4.0$ m/s $G_s = 80.9$ kg/m^2·s $D = 0.30$ m			
Positions of the Probes				Positions of the Probes								Positions of the Probes					
$r = 0$ m $L = 6.60$ m		$r = 0$ m $L = 4.20$ m		$r = 0.149$ m $L = 4.20$ m		$r = 0$ m $L = 6.60$ m		$r = 0$ m $L = 4.20$ m		$r = 0.149$ m $L = 4.20$ m		$r = 0$ m $L = 6.60$ m		$r = 0$ m $L = 4.20$ m		$r = 0.149$ m $L = 4.20$ m	
t	C	t	C	t	C	t	C	t	C	t	C	t	C	t	C	t	C
0.2	0	0.2	0.2	0.3	0	0.1	0	0.1	0	0.4	0	0.2	0	0.2	0.4	0.1	0
0.7	0.3	0.7	0.6	0.4	0.3	0.4	0	0.4	0.6	0.6	0.1	0.5	0.5	0.4	3.6	0.4	0.2
1.2	0.6	1.1	1.0	0.9	1.0	0.7	0.1	0.7	2.1	1.1	0.5	0.9	4.4	0.7	4.8	0.8	1.0
1.7	1.1	1.5	1.3	1.2	1.6	1.0	0.5	1.1	3.3	1.8	1.6	1.3	4.3	1.1	4.1	1.2	2.2
2.3	1.3	2.0	1.4	1.6	2.0	1.3	2.2	1.6	3.5	2.4	2.5	1.6	4.0	1.4	3.6	1.8	2.8
2.9	1.4	2.6	1.1	2.0	1.8	1.6	2.8	2.0	3.2	2.8	2.9	2.0	3.6	1.8	3.5	2.3	2.4
3.4	1.3	3.3	1.1	2.5	1.7	2.0	3.4	2.7	2.7	3.5	3.0	2.5	3.4	2.3	2.7	2.9	2.2
3.9	1.2	3.7	0.8	3.0	1.3	2.3	3.8	3.3	2.2	4.3	2.7	3.0	2.9	2.8	2.5	3.6	1.9
4.4	1.1	4.9	0.6	3.6	1.2	2.7	3.6	4.0	1.5	5.3	1.9	3.5	2.5	3.2	1.8	4.3	1.5
4.9	0.9	6.2	0.4	4.2	1.0	3.0	3.6	4.7	1.1	6.4	1.0	4.1	1.6	3.8	1.2	5.1	1.2
5.4	0.7	7.9	0.2	5.4	0.8	3.4	3.5	5.3	0.8	7.7	0.5	4.8	1.1	4.3	0.8	5.9	0.6
6.0	0.6	10.4	0.1	6.6	0.5	3.8	3.2	5.9	0.6	9.0	0.3	5.5	0.8	5.0	0.6	6.7	0.5
6.7	0.5	13.0	0	8.0	0.3	4.4	2.8	6.8	0.4	10.4	0.1	6.1	0.5	5.7	0.5	7.5	0.5
7.6	0.3	15.7	0	9.9	0.2	5.0	2.0	7.7	0.2	11.9	0	6.7	0.4	6.4	0.4	8.3	0.3
8.6	0.2	18.8	0	11.6	0.1	5.6	1.5	8.4	0.2	13.3	0	7.4	0.3	7.2	0.2	9.2	0.2
9.7	0.1	22.2	0	13.6	0	6.2	1.1	9.4	0.1	14.8	0	8.1	0.2	8.0	0.2	10.2	0.1
10.8	0.1	29.1	0	16.0	0	6.8	1.0	10.4	0.1	17.9	0	8.8	0.2	8.9	0.2	11.0	0.1
12.1	0	—	—	22.2	0	7.6	0.7	11.5	0	19.3	0	9.4	0.1	9.7	0.1	11.9	0.1
13.3	0	—	—	29.3	0	8.3	0.4	12.7	0	20.8	0	10.1	0	10.7	0	12.8	0
14.5	0	—	—	38.0	0	9.5	0.2	14.2	0	—	—	10.7	0	11.8	0	13.6	0
19.3	0	—	—	—	—	10.7	0.1	17.4	0	—	—	13.4	0	12.9	0	14.5	0
22.8	0	—	—	—	—	12.1	0.1	19.7	0	—	—	12.2	0	14.1	0	15.5	0
—	—	—	—	—	—	13.7	0	—	—	—	—	13.0	0	15.5	0	17.7	0
—	—	—	—	—	—	15.2	0	—	—	—	—	—	—	18.9	0	—	—
—	—	—	—	—	—	16.8	0	—	—	—	—	—	—	—	—	—	—
—	—	—	—	—	—	18.3	0	—	—	—	—	—	—	—	—	—	—
—	—	—	—	—	—	20.0	0	—	—	—	—	—	—	—	—	—	—
—	—	—	—	—	—	—	—	—	—	—	—	—	—	—	—	—	—

*C = tracer concentration in mg-NaCl/g-FRF5
t = residence time in seconds

sion of Eq. 1 to each RTD curve using Pe_s as the fitting parameter. Examples of the goodness of fit achieved are shown in Figure 7. It can be seen that the form of the RTD curves is quite adequately described by the simple dispersion model.

To correlate the effect of operating conditions (superficial gas velocity U_o and mean solids flux G_s) and the scale on the longitudinal solids mixing, the more convenient Peclet number, $Pe = (U_o L/D_z)$, derived from Pe_s using Eq. 3 was used. The effect of operating conditions and the scale on longitudinal solids mixing was found to be correlated by the expression:

$$Pe = \left[\frac{U_o L}{D_z}\right] = 9.2D(G_s D)^{0.33} \tag{5}$$

Comparison between Peclet numbers calculated from Eq. 5 and the experimental values is shown in Figure 8. Equation 5 indicates that increasing riser diameter has the effect of decreasing the degree of longitudinal mixing. This agrees with observations of the hydrodynamics of this flow regime, indicating that increasing the diameter of the riser reduces the proportion of downward flowing solids at any position in the riser. Equation 5 also indicates that longitudinal mixing would decrease slightly with increase in mean solids flux G_s. This effect is less straightforward to explain in terms of hydrodynamics. However, there are strong indications that the refluxing transport regime studied here exhibits, over part of its range, a similar profiles condition (Monceaux et al., 1986; Herb et al., 1989, Rhodes et al., 1989), in which the form of radial profiles of reduced solids flux and reduced suspension concentration (local value ÷ cross-sectional mean value) is independent of the solids flux and dictated by the gas velocity. Under these conditions, the solid velocity distribution and, hence, the degree of longitudinal solids mixing would be independent of solids flux. The weak effect of solids flux observed here, therefore, is not greatly at odds with the fluid dynamic observations.

Having correlated longitudinal mixing in terms of the Peclet number in its convenient form Pe, $(U_o L/D_z)$, it is necessary to express the link between median solids velocity $V_{s,0.5}$ and operating conditions to fully describe the solids residence time distribution under any conditions. Over the range of conditions studied, $V_{s,0.5}$ was found to be virtually independent of mean solids flux and to increase in an approximately linear fashion with superficial gas velocity. Figure 9 shows that for a given superficial gas velocity the median solids velocity $V_{s,0.5}$ is always

Table 5. Solids Mixing Data: Experimental Conditions and Results on 0.305-m Rig*

Conditions of Experiment	$U_o = 3.0$ m/s, $G_s = 40.0$ kg/m^2·s, $D = 0.305$ m				Conditions of Experiment	$U_o = 4.0$ m/s, $G_s = 39.7$ kg/m^2·s, $D = 0.305$ m				Conditions of Experiment	$U_o = 5.0$ m/s, $G_s = 39.9$ kg/m^2·s, $D = 0.305$ m			
Positions of the Probes					Positions of the Probes					Positions of the Probes				
$r = 0$ m, $L = 6.60$ m		$r = 0$ m, $L = 4.20$ m		$r = 0.149$ m, $L = 4.20$ m		$r = 0$ m, $L = 6.60$ m		$r = 0$ m, $L = 4.20$ m		$r = 0.149$ m, $L = 4.20$ m		$r = 0$ m, $L = 6.60$ m		$r = 0$ m, $L = 4.20$ m		$r = 0.149$ m, $L = 4.20$ m	
t	C	t	C	t	C	t	C	t	C	t	C	t	C	t	C	t	C
0.1	0	0.2	0	0.2	0	0.1	0	0.2	0	0.2	0.1	0.2	0	0.2	1.1	0.3	0.1
0.3	0	0.5	0.2	0.6	0	0.4	0.3	0.5	0.7	0.7	0.6	0.6	1.2	0.6	3.4	0.8	1.0
0.5	0	0.9	1.4	0.9	0.1	0.7	0.7	0.9	2.5	1.2	1.3	1.1	2.2	1.1	3.9	1.2	1.7
0.8	0.1	1.4	2.5	1.2	0.2	1.1	1.8	1.4	3.4	1.9	2.1	1.5	3.1	1.5	3.9	1.7	2.3
1.1	0.5	1.9	3.1	1.6	0.5	1.6	2.7	2.1	3.6	2.6	2.5	1.9	3.2	2.0	3.4	2.2	3.3
1.4	0.9	2.3	3.3	1.9	0.7	2.1	3.2	2.8	3.1	3.4	3.0	2.3	3.4	2.5	3.4	2.7	3.9
1.6	1.2	2.8	3.2	2.2	1.0	2.6	4.0	3.5	2.3	4.0	2.8	2.8	3.3	2.9	3.2	3.3	3.7
1.9	1.5	3.4	3.2	2.5	1.4	3.2	3.3	4.1	1.7	4.8	2.1	3.5	3.1	3.5	2.7	3.8	3.0
2.2	1.8	4.2	2.3	2.8	1.6	3.8	3.1	4.7	1.3	5.6	1.5	4.2	2.2	4.2	1.8	4.3	2.7
2.7	2.0	5.0	1.8	3.2	1.8	4.4	2.3	5.3	1.0	6.5	1.1	4.9	1.6	4.9	1.4	4.9	2.1
3.4	2.2	5.8	1.5	3.7	2.0	5.2	1.8	5.9	0.8	7.5	0.7	5.7	1.1	5.7	1.1	5.6	1.7
4.2	2.7	6.6	1.2	4.2	1.9	6.0	1.4	6.6	0.6	8.5	0.4	6.4	0.7	6.7	0.7	6.4	1.2
5.0	2.3	7.5	0.8	4.8	2.0	6.8	0.8	7.3	0.3	9.3	0.3	7.2	0.5	7.8	0.4	7.4	0.9
5.7	1.9	8.4	0.6	5.5	2.0	7.7	0.5	8.2	0.3	10.0	0.2	8.2	0.3	9.1	0.3	8.6	0.5
6.5	1.7	9.4	0.3	6.3	1.4	8.8	0.3	9.2	0.1	10.9	0.1	9.3	0.1	10.6	0.2	9.8	0.2
7.2	1.5	10.7	0.2	6.9	1.1	10.0	0.1	10.1	0.1	11.9	0	10.4	0	12.0	0.1	10.9	0.1
8.0	1.0	12.1	0.2	7.5	1.0	11.1	0	11.0	0	13.2	0	11.5	0	13.4	0.1	12.3	0.1
9.0	0.7	13.4	0.1	8.2	0.7	12.2	0	12.1	0	14.5	0	12.8	0	15.0	0	13.8	0
10.5	0.4	14.8	0	9.0	0.5	13.3	0	13.4	0	15.9	0	13.9	0	16.7	0	15.2	0
12.0	0.2	16.3	0	10.0	0.4	14.5	0	14.7	0	17.3	0	15.2	0	18.7	0	16.7	0
13.0	0.1	17.8	0	11.0	0.3	15.7	0	15.9	0	18.8	0	16.5	0	—	—	18.4	0
14.5	0	19.3	0	12.1	0.1	17.1	0	—	—	—	—	—	—	—	—	20.0	—
16.2	0	20.9	0	13.4	0.1	18.5	0	—	—	—	—	—	—	—	—	--	—
17.8	0	22.7	0	14.9	0.1	—	—	—	—	—	—	—	—	—	—	--	—
22.0	0	—	—	16.6	0	—	—	—	—	—	—	—	—	—	—	--	—
24.5	0	—	—	19.0	0	—	—	—	—	—	—	—	—	—	—	--	—
26.8	0	—	—	21.4	0	—	—	—	—	—	—	—	—	—	—	--	—
34.7	0	—	—	—	—	—	—	—	—	—	—						

*C = tracer concentration in mg-NaCl/g-FRF5
t = residence time in seconds

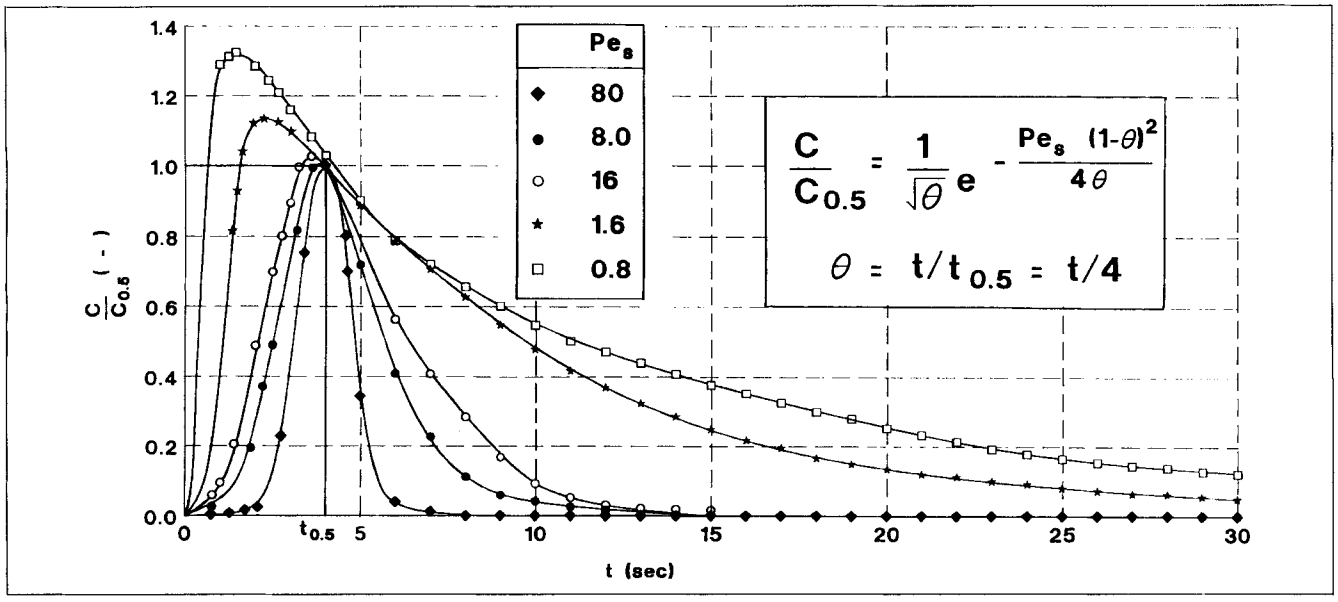

Figure 5. Influence of Peclet number Pe_s on the shape of Solids RTD curve for a median residence time of 4.0 s.

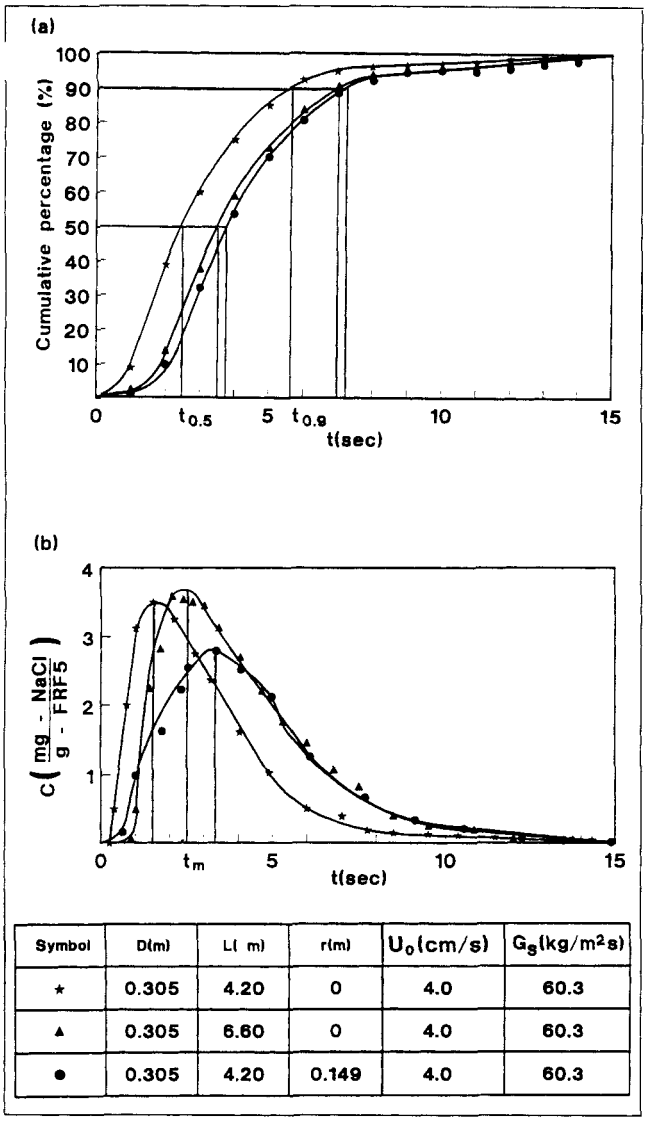

Symbol	D(m)	L(m)	r(m)	U_o(cm/s)	G_s(kg/m²s)
★	0.305	4.20	0	4.0	60.3
▲	0.305	6.60	0	4.0	60.3
●	0.305	4.20	0.149	4.0	60.3

Figure 6. Experimental data on RTD and cumulative wt. % distribution of tracer.

higher in the larger riser than in the smaller one. The following correlations for $V_{s,0.5}$ are derived from Figure 5:

At the riser exit,

$$V_{s,0.5} = 1.21\, D^{0.78} U_o \tag{6}$$

At the axial center,

$$V_{s,0.5} = 0.72\, D^{0.57} U_o \tag{7}$$

Thus, using Eqs. 5, 6 and 7, prediction of residence time distributions and longitudinal dispersion coefficients is possible over the range of operating conditions and the scale studied here. By comparing the RTD curves for tracer particles measured at the axial center of the riser with those measured near the riser wall, some conclusions can be drawn regarding the distribution of particle velocities in the riser. First, by considering the curves in Figure 6b we can deduce that particles

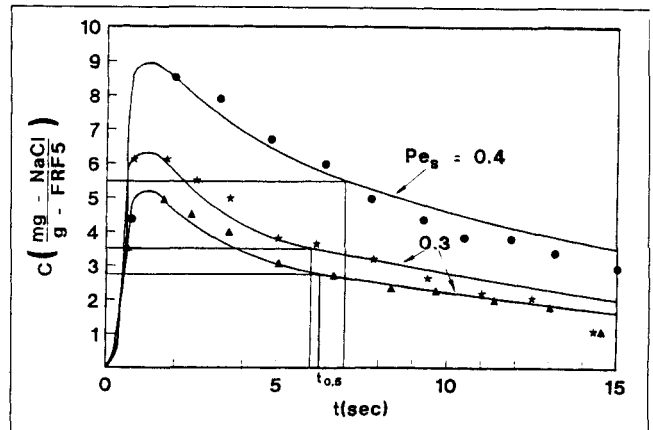

Symbol	D(m)	L(m)	r(m)	G_s(kg/m²s)	U_o(m/s)	$t_{0.5}$(sec)
▲	0.152	4.45	0	10.17	4.01	6.1
★	0.152	6.20	0	10.17	4.01	6.0
●	0.152	4.45	0.073	10.17	4.01	7.0

Figure 7. Predicted RTD curves vs. experimental data.

in the region near the riser wall have greater residence times and a greater range of residence times than those in the axial center of the riser. These results are in accordance with fluid dynamic observations in this flow regime, indicating the existence of a core-annulus structure with higher solids velocities in the core than in the annulus.

Conclusions

Analysis of RTD measurements in the riser of a circulating fluidized bed using an unsteady-state tracer injection method has lead us to the following conclusions:

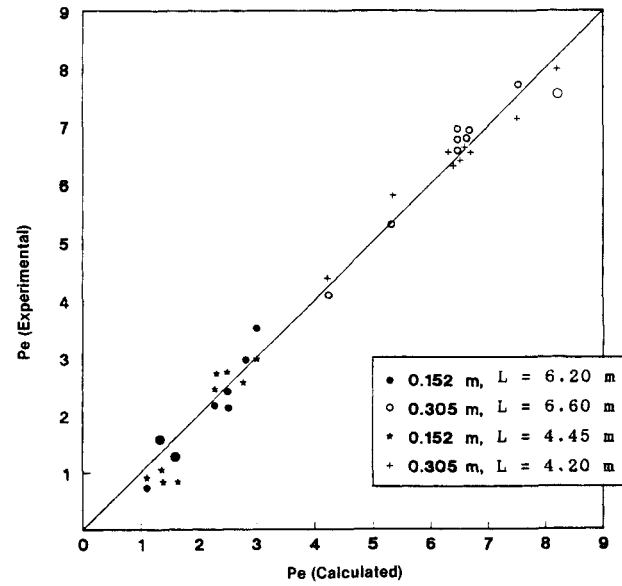

Figure 8. Peclet number $Pe = (U_o L/D_z)$ calculated by Eq. 5 vs. experimental values.

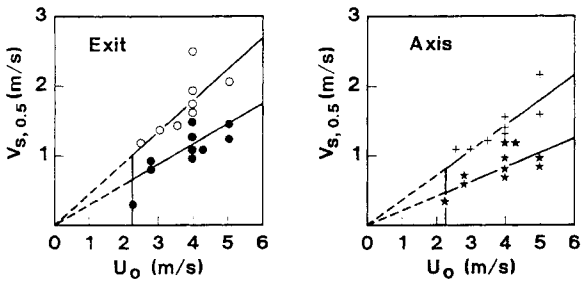

Symbol	D(m)	L(m)	r(m)	G_s(kg/m²s)	Powder
⋆	0.152	4.45	0	5.13-65.4	FRF5
•	0.152	6.20	0	5.13-65.4	FRF5
+	0.305	4.20	0	20.3-80.9	FRF5
○	0.305	6.60	0	20.3-80.9	FRF5

Figure 9. Correlation of median solids velocity $V_{s,0.5}$ with superficial gas velocity U_o.

• A simple, one-dimensional dispersion model is able to satisfactorily describe the measured longitudinal solids mixing over a wide range of operating conditions and for two scales of riser.

• Peclet numbers calculated according to the proposed model are in the range of 1.0–9.0 and are correlated with operating conditions and riser diameter by the expression $Pe = U_o L/D_z = 9.2D\ (G_s D)^{0.33}$ over the range:

$$U_o: \quad 2.8\text{–}5.0 \text{ m/s}$$

$$G_s: \quad 5.0\text{–}80 \text{ kg/m}^2\cdot\text{s}$$

$$D: \quad 0.152 - 0.305 \text{ m}$$

• Over the range of conditions and the scale studied, solids residence time distribution curves may be calculated from a knowledge of mean solids flux, superficial gas velocity, and riser diameter.

• The degree of longitudinal mixing of solids in the riser of a circulating fluidized bed decreases with increasing riser diameter.

• Solids RTD's measured in the riser core and at the riser wall confirm the existence of a core-annulus flow structure, in which solids near the wall have a lower upward velocity than those in the core.

Notation

C = concentration of the salt tracer
C_o = initial concentration (Eq. 1)
$C_{0.5}$ = concentration of the tracer at $t_{0.5}$
D = diameter of the riser
D_z = diffusivity of the salt tracer
G_s = solids circulation flux
L = axial distance from the injector to the sampling point
Pe = Peclet number, $U_o L/D_z$
Pe_s = Peclet number for the solids phase, $LV_{s,0.5}/D_z$
r = radial coordinate
t = residence time
$t_{0.5}$ = median residence time
U_o = superficial gas velocity
$V_{s,0.5}$ = particle velocity of the gravity center for the solids tracer cloud, $L/t_{0.5}$
z = axial coordinate

Greek letters

θ = relative residence time, $t/t_{0.5}$

Literature Cited

Avidan, A. A., "Bed Expansion and Solids Mixing in High Velocity Fluidized Beds," PhD Diss., City College of New York (1980).

Bader, R., J. Findlay, and T. M. Knowlton, "Gas/Solids Flow Patterns in a 30.5-cm-Diameter Circulating Fluidized Bed," *Circulating Fluidized Bed Technology II*, p. 123, P. Basu and J. F. Large, eds., Pergamon Press (1988).

Helmrich, H., K. Schugerl, and K. Janssen, "Decomposition of $NaHCO_3$ in Laboratory- and Bench-Scale Circulating Fluidized Bed Reactors," *Circulating Fluidized Bed Technology*, p. 161, P. Basu, ed., Pergamon Press (1986).

Herb, B., K. Tuzla, and J. C. Chen, "Distribution of Solid Concentrations in Circulating Fluidized Bed," *Fluidization VI*, J. R. Grace, L. W. Schemilt, and M. A. Bergougnou, eds., Engineering Foundation, New York (1989).

Levenspiel, O., and W. K. Smith, "Notes on the Diffusion-Type Model for the Longitudinal Mixing of Fluids in Flow," *Chem. Eng. Sci.*, **6**, 227 (1957).

Monceaux, L., M. Azzi, Y. Molodtsof, and J. F. Large, "Overall and Local Characterisation of Flow Regimes in a Circulating Fluidized Bed," *Circulating Fluidized Bed Technology*, p. 185, P. Basu, ed., Pergamon Press, Oxford (1986).

Rhodes, M. J., "The Upward Flow of Gas/Solid Suspensions: 2. a Practical Quantitative Flow Regime Diagram for the Upward Flow of Gas/Solids Suspensions," *Chem. Eng. Res. Des.*, **67**, 30 (1989).

Yerushalmi, J., and A. A. Avidan, "High Velocity Fluidization," *Fluidization*, p. 226, 2nd ed., J. F. Davidson, R. Clift, and D. Harrison, eds., Academic Press, New York (1985).

Manuscript received June 13, 1991, and revision received Aug. 8, 1991.